Theory of Domain-Wall Structure in Multiple Magnetic Films

Abstract: This paper derives analytically a two-dimensional wall-structure applying to the case of two identical magnetic films separated by a non-magnetic film. It applies also to a variety of other multilayer problems. The calculation is based on the usual micromagnetic principle of energy minimization and all approximations are justified. The wall-structure is found to consist of two "flank" regions, whose shape is governed by anisotropy and stray-field coupling between films, arranged symmetrically about a central "kernel" region whose shape is governed by anisotropy and exchange. In the widely applicable limit of negligible exchange the theory reduces to one given earlier [J. Appl. Phys. 37, 1268 (1966)]. Also included in the discussion are effects of quasi-walls and film-to-film exchange interactions. Existing experimental data on wall-shape confirm the shape of the kernel but are not of sufficient precision to test the shape of the flanks. Existing data for permalloy suggest that perpendicular anisotropy may play a significant role in reducing multiple-film wall energy and thickness.

1. Introduction

The term multiple magnetic film refers to configurations of two or more ferromagnetic films separated by nonmagnetic films that are thick enough and uniform enough for the exchange coupling between magnetic films to be weak or negligible, but are thin enough for stray-field interaction between films to be appreciable. Early work on coercivity and other domain-wall effects in double films demonstrated that appropriate circumstances could lead to appreciable domain-wall interaction between the two magnetic films.1-4 To explain the reduced coercivity of multiple films, Clow proposed that in a multiple film Néel walls lie one above the other in such a way that the magnetization within each wall is antiparallel to the magnetization within the neighboring walls.2 The much reduced wall energy serves to account for the reduced coercivity of a multiple film as compared to that of a single film.

In later work, calculations showed that the stray-field interaction between walls in separate films is strong enough to alter by orders of magnitude the shape and energy of these walls if the non-magnetic intermediate layer is sufficiently thin.⁵⁻⁸ In fact, that work showed that the interaction is capable of stabilizing a Néel-like structure (magnetization M parallel to film plane) in films whose thickness is in the Bloch-wall (M perpendicular to wall normal) range for single films. Moreover, Middelhoek showed that the propensity for flux closure is so great that if there is a true wall in only one film it may induce in the second film a disturbance (called a quasi-wall) separating two like-magnetized domains.⁵ These circumstances were

found to give rise to domain structures not existing in single films, ^{5,9-11} and to a reduction of coercive field when the intermediate layer is SiO. ^{2,5,9} Feldtkeller showed how the additional influence of a film-to-film exchange-like interaction, present when the intermediate layer is a metal, gives rise to an increase in coercivity. ⁷ Patton and Humphrey measured mobilities of double walls. ¹²

At this stage, theoretical models for double-film walls assumed that M is everywhere exactly parallel to the film plane.⁵⁻⁸ The dependence of **M** on position was described by an assumed function of one form or another containing a wall-thickness parameter which was determined variationally. A less restrictive but still simple calculation allowed a small component of M to exist normal to the film plane, thus allowing a further reduction of stray-field energy.¹³ The dominant energy terms were still stray-field and anisotropy; exchange was of secondary importance. The shape of the wall was calculated rather than assumed, and the component of M perpendicular to the wall plane was found to vary exponentially with position. 13 Reviews of double-film physical properties have been given by Middelhoek,14 who includes very simple and essentially correct estimates of thickness and energy, and by Feldtkeller.15

The present paper presents a calculation of the wall shape in a double film which we believe to be satisfactory from the micromagnetic point of view. Although the method of solution is improvised, rather than a head-on solution of micromagnetic field equations, ¹⁶ we offer arguments to show that our approximation errors are

really of higher order. An essential element in the calculation is to allow **M** to vary in two dimensions rather than one as in the usual wall calculations.

We show that in the absence of "perpendicular anisotropy" (see the paragraph below) the normal component of magnetic field **H** penetrates into the film a distance x which is typically very small (about 40 Å in permalloy). Since the other components of **H** are of higher order, it follows that the stray-field energy density $(H^2/8\pi)$ resides predominantly in the non-magnetic layer between the films. The wall thickness and energy are determined mainly by a balance of in-plane uniaxial anisotropy K and stray-field forces; the exchange A plays a secondary role under the usual experimental conditions. (The same conclusion was drawn from our earlier sketchy argument. ¹³) In any case, however, as we show here, A and K are the predominant forces determining the wall shape in a narrow region about the center of the wall.

The term "perpendicular anisotropy" refers to a phenomenological dependence of internal energy on the component of **M** perpendicular to the film plane. Experiments of Fujiwara *et al.* have shown that, depending on conditions of preparation, the coefficient for this effect may be quite large in Ni-Fe alloy films. Our calculations here show that the experimental values are large enough for perpendicular anisotropy to have a serious influence on wall shape and energy.

The contents of the paper are organized as follows. In Section 2 we formulate the variational problem in terms of two-dimensional H and M distributions, and then express H approximately in terms of M, reducing the problem to a distribution of M in two dimensions. In Section 3 we reduce the two dimensions to one, expressing all the film-tofilm coupling by means of an effective anisotropic exchange energy term proportional to a single coupling coefficient μ. In Section 4 we calculate an exact solution of the Euler equation for the reduced problem, thus giving formulas for the shape and energy of the wall. In Section 5, we discuss the following points: wall shape, its relationship to previous calculations, validity of our approximations, comparison with experiment, effects of perpendicular anisotropy, quasi-walls, extensions to three or more magnetic films, and the incorporation of exchange-like coupling between films.

2. Elimination of H

In this section we formulate the two-dimensional micromagnetic field problem for a double wall in a pair of identical magnetic films separated by a non-magnetic layer. The problem is first stated in terms of the field variables H and M in two dimensions. By making reasonable approximations we will eliminate H, thus reducing the problem to a determination of M in two dimensions.

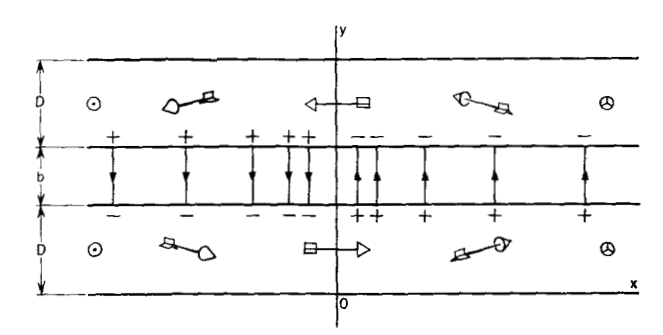


Figure 1 Coordinate system for a double film. The schematic magnetic configuration is for a double true-wall of the first kind. Arrows within magnetic layers of thickness D indicate direction of magnetization (in perspective). Arrows in non-magnetic gap indicate magnetic field.

Figure 1 shows a section of two plane-parallel magnetic films with spontaneous magnetization $|\mathbf{M}| = M_0$, each with thickness D, and separated by a non-magnetic layer of thickness b. A boundary region centered about the y-z plane is assumed to separate semi-infinite domains magnetized in the $\pm z$ directions as indicated in the figure. The x-z plane is assumed to lie on the lower surface of the lower film.

The energy density & of such a system may be written

$$\mathcal{L} = (H^2/8\pi) + (A/M_0^2) \times (\nabla \mathbf{M})^2 + kM_x^2 + k_{\perp}M_y^2.$$
 (1)

The first term in Eq. (1) is the energy density due to the magnetic field **H** which satisfies the equations

$$\nabla \times \mathbf{H} = 0, \tag{2}$$

and

$$\nabla \cdot (\mathbf{H} + 4\pi \mathbf{M}) = 0. \tag{3}$$

In addition, the normal component of $\mathbf{H}+4\pi\mathbf{M}$ is continuous at all surfaces of discontinuity and, since we assume zero applied field, $\mathbf{H}\to 0$ as $|x|\to \infty$ or $|y|\to \infty$. The second term in Eq. (1) is the exchange energy in the continuum limit, with A the conventional exchange constant. The third term represents an anisotropy which is equivalent to the usual in-plane uniaxial anisotropy as long as $M_y=0$. Since we assume the z-axis to be the easy direction the coefficient k is positive and is related to the conventional K by the equation

$$k = K/M_0^2. (4)$$

The first three terms of Eq. (1) have all been considered in previous theories of walls in multiple films.^{5-8,13}

Because it has an important effect on the wall structure, we include here, in addition, the perpendicular anisotropy term appearing last in Eq. (1). Its existence was first pro-

posed in order to account for "stripe domains" in single films of permalloy.¹⁷ Perpendicular anisotropy was later measured directly by Fujiwara *et al.* in a torque balance.¹⁸ Our coefficient k_{\perp} is related to K_{\perp} of Fujiwara *et al.* by

$$K_{\perp} = -k_{\perp} M_0^2 - 2\pi M_0^2. (5)$$

We should note here that the mathematical expression of Fujiwara *et al.* for perpendicular anisotropy includes the shape anisotropy due to the plane geometry. In our case shape anisotropy is effectively included in $(H^2/8\pi)$ and not in $k_\perp M_\nu^2$.

Our notation might be objected to on the grounds that the in-plane uniaxial anisotropy is properly $k(M_x^2+M_\nu^2)$ so that k_\perp as defined includes in-plane as well as out-of-plane anisotropy. However, in practice the ambiguity is of little consequence because typically $|k_\perp| \gg |k|$. Since the definitions here are more convenient for our purposes we will adhere to them.

Formally speaking, the problem is to minimize the integral of \mathcal{L} over all volume under the constraints of Eqs. (2) and (3) and

 $\mathbf{M} \cdot \mathbf{M} = M_0^2$, for y within magnetic film;

$$= 0$$
, for y not within magnetic film. (6)

We will minimize the energy subject to the six assumptions listed below. The resulting wall structure will turn out to be internally consistent with respect to these assumptions (except for Assumption 4, below, which we do not test) as long as the film parameters obey certain bounds derived in Section 5.

Assumption 1. The solution M(x, y, z) has the highest symmetry consistent with that of the boundary conditions and qualitative energy considerations.

The symmetry about the planes x = 0 and y = D + b/2 is apparent in Fig. 1. To be explicit, M_x is even, and M_y and M_z are odd with respect to reflection in the y-z plane. Also, M_x is odd, and M_y and M_z are even with respect to reflection in the plane y = D + b/2. In addition all field quantities are independent of z. One can see from the figure that the assumed symmetry for M_x and M_y tends to facilitate flux closure.

Assumption 1 precludes structures (such as cross-tie walls in single films)¹⁹ in which M varies in the z-dimension as well. The possibility of such solutions with symmetry lower than the symmetry of the boundary conditions lurks because of the "non-linear" constraint of (6) but will be neglected in our work. The assumed symmetry allows us to confine explicit calculations to the region $x \ge 0$, $y \le D + b/2$, from which the remaining regions are determined by reflection in the symmetry planes.

Assumption 2. M_y^2 is much less than M_0^2 .

This condition is suggested by the fact that the shape anisotropy of a magnetic film tends to suppress the normal component of magnetization. In earlier work on multiple films it was assumed to vanish altogether, as in a single-film Néel wall. However, we find a decided decrease in energy by allowing M_v to be finite. By Assumption 2, the constraint of (6) becomes

 $M_r^2 + M_s^2 = M_0^2$, for y within magnetic film;

$$\mathbf{M} \cdot \mathbf{M} = 0$$
, for y not within magnetic film, (7)

and M_y is an independent variable within the magnetic film. We may define the in-plane angle ϕ by the equations

$$M_z = M_0 \cos \phi, \qquad M_z = M_0 \sin \phi. \tag{8}$$

The angle ϕ serves as an independent variable in place of M_z and M_z .

Assumption 3. All field quantities vary slowly with x on a scale measured by D + b.

Assumption 4. The angle ϕ depends on x but not on y within a given film.

This assumption is suggested by the fact that the boundary conditions are (partly according to Assumption 1)

$$\phi = 0$$
 at $x = 0$, and $\phi = \pm \pi/2$ at $x = \pm \infty$, (9)

respectively, for all y within the lower film of Fig. 1. Permitting ϕ to vary with y would contribute to exchange energy. Given the fact of (9) that ϕ does not depend on y at the boundaries, and given the thinness of the films according to Assumption 3, it is difficult to see what energy terms might be decreased in compensation for the increase in exchange if ϕ were allowed to vary with y. Nonetheless, since we do not actually calculate the conditions under which Assumption 4 is satisfied we regard it as the unproved premise on whose validity the correctness of the calculation hinges.

However, we must not attempt to employ the same argument to neglect the y-dependence of M_y . The relevance of the function $\partial M_y/\partial y$ to the magnetic field energy is apparent from Eq. (3). In our previous simple calculation, ¹³ we showed that the pole density contributed by $\partial M_y/\partial y$ may be employed to effectively displace the pole density arising from dM_x/dx within the magnetic films to the inner surfaces. The poles were thus placed as close as possible to their partners of opposite sign across the gap so as to minimize magnetic field energy. In the present paper we calculate $M_y(x, y)$ in greater detail.

Assumption 5. The quantity $(H^2/8\pi)$ external to the film sandwich is negligible, both with respect to energy and continuity of $H_y + 4\pi M_y$ at the boundaries y = 0, b + 2D.

This assumption is suggested by Assumption 3 together with the resemblance of the problem to that of a parallel-plate capacitor. The analogy also suggests that the internal component H_x for points within the magnetic films and the gap is negligible. This is easily proved as follows. The

magnetic potential ψ satisfies the equation

$$\mathbf{H} = -\nabla \psi. \tag{10}$$

We may take $\psi = 0$ on symmetry planes y = b/2 + D and x = 0 by Assumption 1. Then ψ may be evaluated by means of the line integral

$$\psi(x, y) = -\int_{b/2+D}^{y} dy' H_{y}(x, y')$$
 (11)

so that $|\psi|$ is of the order $|H_y|$ (D+b) within the sandwich. It follows that $|H_x|=|\partial\psi/\partial x|$ is of the order $|H_y|(D+b)/a$ where a is the width of the wall. By Assumption 3, (D+b)/a is small and H_x^2 may be neglected in comparison with H_y^2 .

By extension of this reasoning $|\partial H_x/\partial x| \ll |\partial H_y/\partial y|$. Therefore, by Assumption 4, Eq. (3) reduces to

$$H_{y,y}(x, y) + 4\pi M_{y,y}(x, y) + 4\pi M_{x,x}(x) = 0 (0 \le y \le D), (12)$$

where we use the notation $H_{y,y} \equiv \partial H_y/\partial y$, etc. and where we have defined $M_x(x) \equiv M_x(x, y)$ for $0 \le y \le D$.

In order to find **H** with sufficient accuracy to calculate energy for a given distribution of **M** we need only to integrate Eq. (12). We have

$$H_{\nu}(x, y) + 4\pi M_{\nu}(x, y)$$

 $+ 4\pi y M_{x,x}(x) = f(x), \qquad (0 \le y \le D), \qquad (13)$

where f(x) is a function to be determined. Both H_y and M_y vanish for y < 0 (Assumption 5). Since the normal component of $\mathbf{H} + 4\pi \mathbf{M}$ must be continuous at any boundary, $H_y + 4\pi M_y$ must vanish as y approaches zero from the positive side. This condition substituted in Eq. (13) shows that

$$f(x) = 0. (14)$$

In particular we find that on the upper surface of the lower magnetic film

$$H_{\nu}(x, D) + 4\pi M_{\nu}(x, D) = -4\pi D M_{x,x}(x),$$
 (15)

so that the field in the gap is simply

$$H_{\nu}(x, y) = -4\pi D M_{\tau, \tau}(x), (D < y < D + b).$$
 (16)

Assumption 6. $(A/M_0^2)M_{\nu,z}^2$ in Eq. (1) can be neglected when calculating the volume integral of \mathcal{L} .

Equation (1) for the energy density may now be reduced to a simpler form. Within the lower film it becomes, according to our assumptions and Eqs. (13) and (14),

$$\mathcal{L} = 2\pi [M_{\nu}(x, y) + y M_{x,z}(x)]^{2}$$

$$+ (A/M_{0}^{2})[M_{x,z}^{2}(x) + M_{x,z}^{2}(x) + M_{\nu,\nu}^{2}(x, y)]$$

$$+ k M_{x}^{2}(x) + k_{\perp} M_{\nu}^{2}(x, y) \qquad (0 \le y \le D). \qquad (17)$$

Within the gap, Eq. (1) becomes, according to Eq. (16),

$$\mathcal{L} = 2\pi D^2 M_{x,x}^2(x) \qquad (D \le y \le D + b). \tag{18}$$

In these equations **H** has been effectively eliminated as a field variable. The remaining independent variables are $M_{\nu}(x, y)$ and $\phi(x)$, the latter by virtue of Eq. (8).

3. Reduction to one dimension

Here we proceed to reduce the two-dimensional energy density given by Eqs. (17), (18), and (8) to one dimension by integrating over y. The resulting problem will resemble the elementary Bloch-wall problem.

We may write the Euler equation for M_{ν} ,

$$\frac{\partial \mathcal{L}}{\partial M_{y}} - \frac{\partial}{\partial x} \left(\frac{\partial \mathcal{L}}{\partial M_{y,x}} \right) - \frac{\partial}{\partial y} \left(\frac{\partial \mathcal{L}}{\partial M_{y,y}} \right) = 0. \tag{19}$$

After substitution of Eq. (17), this becomes

$$(2A/M_0^2)M_{y,\nu\nu}(x,y) - (4\pi + 2k_\perp)M_{\nu}(x,y)$$

= $4\pi y M_{x,\nu}(x)$ $(0 \le y \le D)$. (20)

For the present, we consider x to be a parameter and $M_x(x)$ to be a given function. Then Eq. (20) is an ordinary linear differential equation for M_y with the independent variable y. The general solution is

$$(4\pi + 2k_{\perp})M_{y} = \Lambda(x)e^{y/\lambda} + \Gamma(x)e^{-y/\lambda} - 4\pi y M_{x,x}(x),$$
(21)

where the functions $\Lambda(x)$ and $\Gamma(x)$ are to be determined, and where

$$\lambda^2 = A[(2\pi + k_\perp)M_0^2]^{-1}. \tag{22}$$

A boundary condition following from the variational principle is that the normal gradient of **M** vanishes at a magnetic-nonmagnetic interface if surface anisotropy is neglected. In the present instance this condition becomes

$$M_{v,v}(x, 0) = M_{v,v}(x, D) = 0.$$
 (23)

Application of this condition to Eq. (21) determines the functions Λ and Γ so that finally

$$(2\pi + k_{\perp})M_{y} = 2\pi M_{x,x} \{-y + \lambda(1 + e^{D/\lambda})^{-1} \times [e^{y/\lambda} - e^{(D-y)/\lambda}]\} \qquad (0 \le y \le D).$$
 (24)

We note in passing the magnetic field within the magnetic layers, obtained by substituting this equation into Eq. (13):

$$H_{y} = \frac{4\pi M_{x,x}}{2\pi + k_{\perp}} \left\{ -k_{\perp} y - \frac{2\pi \lambda \left[e^{y/\lambda} - e^{(D-y)/\lambda} \right]}{1 + e^{D/\lambda}} \right\} \cdot (25)$$

The field within the gap has already been given by Eq. (16). The dependence of M_y on y given by Eq. (24) is plotted in Fig. 2a. If $D \gg \lambda$, this function is linear within the film except at points within boundary layers of thickness of the order λ adjoining all surfaces.

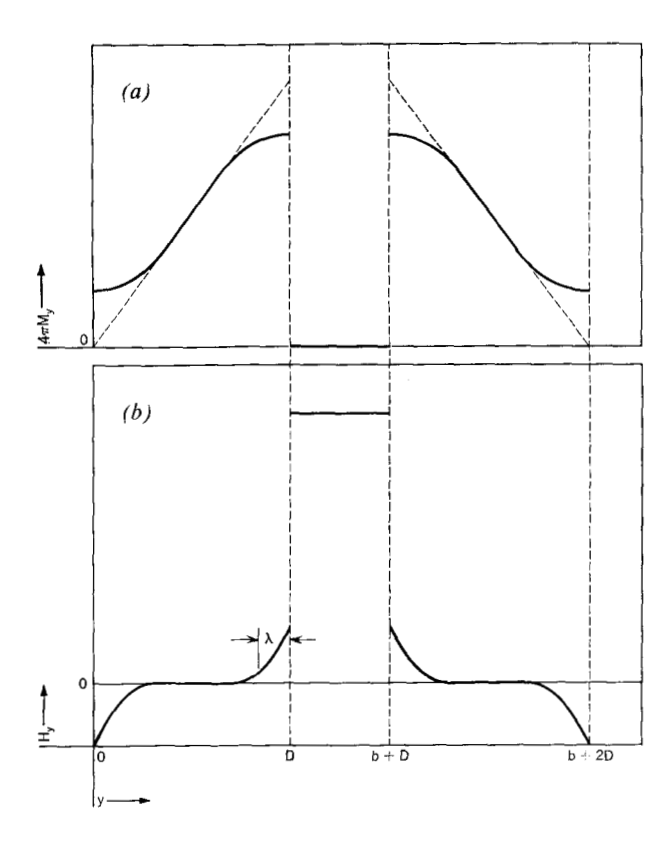


Figure 2 Schematic plots of (a) M_{ν} and (b) H_{ν} versus y for constant x and vanishing perpendicular anisotropy. The meaning of the shielding length λ is indicated in (b) as the depth to which H_{ν} penetrates the magnetic film.

In the special case $k_{\perp}=0$, one finds that the pole density $-\nabla \cdot M$ vanishes in the linear region and is non-vanishing within the boundary layers. On the outer magnetic surfaces at y=0 and y=b+2D, there are surface distributions of poles, each of which is equal and opposite to the integrated volume pole distribution within the adjoining boundary layer. Thus the field distribution due to the poles on outer boundary layers is completely internal to the respective layers, as shown in Fig. 2b sketched from Eqs. (16) and (25).

The pole distributions residing on the inner magnetic surfaces at y = D and y = b + D have the same signs as the respective adjoining boundary-layer distributions. These provide sources for the field **H** within the gap as well as the boundary layers themselves. The result is that in the special case $k_{\perp} = 0$ the magnetic energy density $(H^2/8\pi)$ resides within the gap and boundary layers, and contributions from the bulk of the magnetic material are negligible for sufficiently great thickness.

The quantity λ is seen to represent a shielding depth within which the normal component of **H** is permitted to penetrate by virtue of exchange. A volume distribution of

poles on a scale greater than λ cannot exist within the magnetic film because of the shielding effect due to the infinite y-component of susceptibility implied by $k_{\perp}=0$. For typical permalloy parameters ($A=10^{-6}$ erg/cm and $M_0=800$ emu) we find that λ is about 40 Å. We must remark that this concept has a limited significance because if k_{\perp} does not vanish some field penetrates beyond the boundary layer, as is evident from Eq. (25).

We resume consideration of a general value of k_{\perp} . In order to reduce the problem to one dimension we write the energy density g averaged over the thickness of the magnetic layers:

$$g(x) = D^{-1} \int_0^{D + \frac{1}{2}b} \mathfrak{L}(x, y) dy.$$
 (26)

The integrand of this equation is evaluated within the region 0 < y < D by substitution of Eqs. (8) and (24) into Eq. (17). Within the region $D < y < D + \frac{1}{2}b$ the integrand is given by Eq. (18). The integral reduces to a combination of elementary exponential integrals. Upon carrying through the integration and simplifying we find the result:

$$g = K \cos^2 \phi + A(d\phi/dx)^2 + \mu(d \cos \phi/dx)^2$$

= $K \cos^2 \phi + (d\phi/dx)^2 (A + \mu \sin^2 \phi),$ (27)

where the coupling coefficient μ is given by

$$\mu = \pi b D M_0^2 + \left[2\pi/(2\pi + k_\perp) \right]^2$$

$$\times A[1 - (2\lambda/D) \tanh(D/2\lambda)]$$

$$+ 2\pi k_\perp D_0^2 M_0^2 / [3(2\pi + k_\perp)], \qquad (28)$$

in which λ is the skin depth defined by Eq. (22). Thus we see that the energy density contains the usual anisotropy and exchange terms appearing in the Bloch wall problem for bulk material, plus an additional coupling term $\mu(d\cos\phi/dx)^2$ which takes into account all stray-field and other effects arising from the double-film geometry.

Let us recapitulate the significance of the coefficient μ . The first term in Eq. (28) is due to the stray-field energy in the gap. The second and third may be considered to arise predominantly from exchange and perpendicular anisotropy, respectively, contributed by tilting **M** out of the film plane. However both terms involve the effect of demagnetization and the second is influenced by perpendicular anisotropy, too. The *tanh* expression appearing within the second term brings into account the energy improvement which comes about when **H** is permitted to penetrate into the skin of thickness λ .

We note that unless k_{\perp} is sufficiently large and negative, μ is positive. The coupling term in the energy represents an effective anisotropic exchange energy contributed by M_z but not by M_z . Hence, we see that the qualitative effecs of the coupling energy must be to reinforce the exchange effect (if $\mu > 0$) and thus to increase wall thickness and energy beyond the bulk values of these quantities.

4. Solution of the reduced problem

In the previous sections we have expressed the average energy density g, given in Eq. (27), in terms of a single space variable x. The energy per unit wall area is

$$W = \int_{-\infty}^{\infty} g(\phi, \phi') dx, \qquad (29)$$

where $\phi' \equiv d\phi/dx$. This expression must be minimized with respect to the wall shape $\phi(x)$ to obtain the stable wall configuration. A first integral of the Euler equation obtained by variation of W may be derived by following the same procedure used in deriving the law of conservation of energy from Lagrange's equation[†] because, according to Eq. (27), g does not depend explicitly on x. The result is

$$g - \phi' \frac{\partial g}{\partial \phi'} = 0. {30}$$

This equation may be used to express ϕ' in terms of ϕ . Substituting Eq. (27) into Eq. (30) and solving, we find

$$\phi'^{2} = K \cos^{2} \phi / (A + \mu \sin^{2} \phi). \tag{31}$$

The wall energy γ_p may be calculated without solving for $\phi(x)$ since

$$\gamma_p = W_{\min} = \int_{-\pi/2}^{\pi/2} g \phi'^{-1} d\phi.$$
 (32)

Substituting Eqs. (27) and (31) into Eq. (32) we find

$$\gamma_{p} = 2K^{\frac{1}{2}} \int_{-\pi/2}^{\pi/2} (A + \mu \sin^{2} \phi)^{\frac{1}{2}} \cos \phi \, d\phi$$

$$= 4K^{\frac{1}{2}} \int_{0}^{1} (A + \mu u^{2})^{\frac{1}{2}} \, du, \qquad (33)$$

where $u = \sin \phi$. In integral tables one finds the result:

$$\gamma_{p} = 2K^{\frac{1}{2}}(\mu + A)^{\frac{1}{2}} + 2A(K/\mu)^{\frac{1}{2}} \times \ln\left[(\mu/A)^{\frac{1}{2}} + (1 + \mu/A)^{\frac{1}{2}}\right].$$
(34)

To calculate the wall shape, we write, from Eq. (31),

$$K^{\frac{1}{2}}dx = d\phi (A + \mu \sin^2 \phi)^{\frac{1}{2}}/\cos \phi. \tag{35}$$

Making the change of variable $u = \sin \phi$, this becomes

$$K^{\frac{1}{2}}dx = du(A + \mu u^{2})^{\frac{1}{2}}/(1 - u^{2}), \tag{36}$$

in which the integral of the right hand side is given directly by tables. The result is

$$K^{\frac{1}{2}}x = \frac{1}{2}(\mu + A)^{\frac{1}{2}} \ln \left\{ \frac{(\mu u^{2} + A)^{\frac{1}{2}} + (\mu + A)^{\frac{1}{2}}u}{(\mu u^{2} + A)^{\frac{1}{2}} - (\mu + A)^{\frac{1}{2}}u} \right\} - \mu^{\frac{1}{2}} \ln \left\{ A^{-\frac{1}{2}} [\mu^{\frac{1}{2}}u + (\mu u^{2} + A)^{\frac{1}{2}}] \right\}, \quad u = \sin \phi, \quad (37)$$

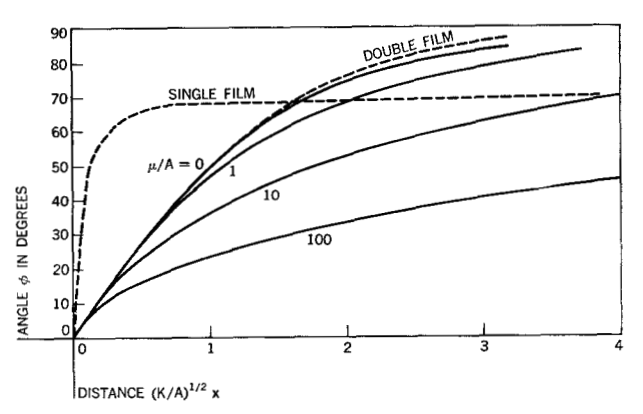


Figure 3 Wall shapes in a double film. The angle ϕ between M and the z axis is plotted as a function of the dimensionless position $(K/A)^{1/2}x$, for various values of the parameter ratio μ/A . The broken curves represent experimental data taken from Ref. 21.

under the condition $\mu + A > 0$, as may be verified by differentiation.

5. Discussion

Wall shape

The main results of this paper are embodied in Eqs. (8), (24), and (37) for the shape of the wall and in Eq. (34) for the energy of the wall, with the necessary definitions of λ and μ being given in Eqs. (22) and (28). In Fig. 3 we plot the angle ϕ as a function of the reduced coordinate $K^{\frac{1}{2}}x/A^{\frac{1}{2}}$ for several values of the reduced coupling coefficient μ/A . For $\mu/A=0$ the shape reduces to that of a Bloch wall in bulk, given by

$$\sin \phi = \tanh \left[(K/A)^{\frac{1}{2}} x \right]. \tag{38}$$

except, of course, that the wall is Néel-like rather than Bloch-like with respect to the plane containing M. For larger values of μ/A , the shape follows closely the bulk solution for small x but "breaks away" at larger x to give a greater total wall width. The bulk-like behavior for small x follows from the fact that in this region (called the "kernel") M_x is nearly equal to M_0 so that first-order rotation of M changes M_x only in second order. Since the surface pole density (proportional to $M_{x,x}$) is small, the demagnetizing energy is likewise, and so the behavior reduces to bulk-like.

The case $\mu \gg A$ is often of experimental interest. In this case wide "flanks" become distinguished from the narrow bulk-like kernel. The flank regions satisfy the inequality

$$\mu \sin^2 \phi \gg A, \tag{39}$$

in which case Eq. (37) reduces to

$$\cos \phi = \exp \left[-(K/\mu)^{\frac{1}{2}} x \right]. \tag{40}$$

[†] See, for example, H. Goldstein, Classical Mechanics, Addison-Wesley, 1953, Section 2-6.

On the other hand, the kernel region satisfies the inequality

$$\mu \sin^2 \phi \ll A, \tag{41}$$

leading to Eq. (38). The width of the flank is of the order $(\mu/K)^{\frac{1}{2}}$ whereas that of the kernel is of the order $(A/\mu)^{\frac{1}{2}}(A/K)^{\frac{1}{2}}$. The ratio of flank-to-kernel is then μ/A . Also the energy in Eq. (34) reduces, when $\mu \gg A$, to

$$\gamma_{P} = 2(K\mu)^{\frac{1}{2}}. \tag{42}$$

• Relationship to previous calculations

It was the limit $\mu \gg A$ to which our previous results were confined.¹³ In that case, if k_{\perp} is neglected, Eq. (28) reduces to

$$\mu = \pi b D M_0^2, \tag{43}$$

which, when substituted in Eqs. (40) and (42), recovers our previous results.¹³ Middelhoek has given a simple estimate of γ_p which is a factor $\sqrt{2}$ larger than that given by Eqs. (42) and (43).¹⁴

Our still earlier joint work⁶ neglected M_{ν} . Within the limitations of the x-dependence assumed therein the results were for this reason correct only in the limit $D/b \ll 1$. Calculations by Feldtkeller⁷ and Friedlaender and Silva⁸ of double-wall energy also neglect M_{ν} and assume arbitrary wall shapes. A summary of all previous results and their genesis is given by Middelhoek.¹⁴

In retrospect we can see that the trial-function method based on a one-parameter trial function cannot represent the double-film wall generally, because here we find two kinds of region, kernel and flanks, which require two parameters to characterize. However, the results of all of References 6-8 mentioned above are approximately correct in the limit $b\gg D$, $A\ll\mu$, $k_\perp=0$. In this limit they do not have the correct detailed wall shape but they give, within a factor of the order of unity, the correct energy and wall width as represented by Eqs. (40), (42), and (43) (which, however, are not limited to the case $b\gg D$). Each of those references contains a factor $(b+\frac{2}{3}D)^{\frac{1}{2}}$ in the energy which is more properly $b^{\frac{1}{2}}$, according to our present results.

• Validity of approximations

In Section 2 a series of assumptions was made with partial justification. In the present section we test the calculated wall structure for consistency with these assumptions. We will argue that the condition of large wall thickness, namely,

$$(\mu/K)^{\frac{1}{2}} + (A/K)^{\frac{1}{2}} \gg b + D,$$
 (44)

is sufficient to guarantee internal consistency and we will establish the range of film parameters that satisfy it.

Assumption 1. The assumed symmetry is seen to be satisfied by the **M** generated from our solution given in the half-plane $y \le D + b/2$, by reflecting it about this boundary. All field variables have the required continuity properties except in the limit $A \to 0$ when discontinuities appear on the plane x = 0, but these we will find to be energetically negligible in connection with other assumptions to be discussed below.

Assumption 2. An upper bound on $|M_y|$ is obtained from the calculated structure by noting that, according to Eq. (24).

$$|(2\pi + k_{\perp})M_{\nu}| < 2\pi |M_{x,z}| D = 2\pi M_0 D |\phi' \sin \phi|.$$

From Eq. (31) the calculated structure also satisfies the inequalities

$$|\phi' \sin \phi| < (K/\mu)^{\frac{1}{2}} \text{ and } |\phi' \sin \phi| < (K/A)^{\frac{1}{2}},$$

for $\mu > 0$. Combining these two inequalities we have

$$|(2\pi + k_{\perp})M_{\nu}/2\pi M_0| < D(K/\mu)^{\frac{1}{2}}$$
, and

$$|(2\pi + k_{\perp})M_{\nu}/2\pi M_0| < D(K/A)^{\frac{1}{2}}.$$

Therefore, if k_{\perp} is not close to -2π , $\mu > 0$, and condition (44) is satisfied, then the calculated structure is consistent with Assumption 2.

Nonetheless, Assumption 2 merits further discussion because we shall see that the calculated structure in the limit $A \rightarrow 0$ has discontinuities on the plane x = 0, if we require the exact constraint (6) to be satisfied. To this end we write the equations

$$M_x = (M_0^2 - M_y^2)^{\frac{1}{2}} \cos \phi, \tag{45}$$

anc

$$M_{\star} = (M_0^2 - M_{\nu}^2)^{\frac{1}{2}} \sin \phi, \tag{46}$$

which satisfy the exact constraint (7), in place of Eq. (8). Now we assume $\lambda = 0$ and $k_{\perp} = 0$ for simplicity and substitute our calculated structure $\phi(x)$, $M_{\nu}(x, y)$, as given by Eqs. (24) and (37), into Eqs. (45) and (46) to find the limiting values on the plane x = 0 given in Table 1. We see that both M_x and M_{ν} are discontinuous at x = 0 in the limit $A \to 0$.

Table 1. Values of M in the limit $A \to 0$, displaying discontinuities at the plane x = 0, for y in the range $0 \le y \le D$, shown for the special case $\lambda = 0$, $k_{\perp} = 0$.

	x = 0	x = 0	$x = 0^+$
M_x	$(M_0^2 - M_y^2)^{\frac{1}{2}}$ $2\pi M_0 (K/\mu)^{\frac{1}{2}} y$	M_0	$(M_0^2 - M_\nu^2)^{\frac{1}{2}}$
M_{ν}	$2\pi M_0(K/\mu)^{\frac{1}{2}}y$	0	$-2\pi M_0(K/\mu)^{\frac{1}{2}}y$
M_z	1	0	0

In order to show that these discontinuities are energetically negligible we estimate the corresponding energy corrections before taking the limit $A \to 0$. First, we consider exchange energy. Since the discontinuity in M_x is second order in that of M_v , the dominant exchange correction comes from the term $AM_{y,x}^2/M_0^2$. This term was neglected altogether in Assumption 6, and will be evaluated below in connection with the review of that assumption. The singular corrections to anisotropy are easily seen to vanish because M_v and M_x are bounded; only their derivatives are not.

We are then left with the need to consider a correction to stray-field energy. Let \mathbf{M}_c be the correction to \mathbf{M} . Then, expanding the radical in Eq. (45), we have

$$\nabla \cdot \mathbf{M}_c = -(M_{\nu} M_{\nu,x}/M_0) \cos \phi - (M_{\nu}^2/2M_0) \phi' \sin \phi. \tag{47}$$

The contribution of the second term is seen to be negligible by noting that it gives only a small correction to the calculation of H_{ν} from Eq. (12). Neglecting λ/D , we have from Eq. (24),

$$M_{\nu} = y M_0 \phi' \sin \phi, \tag{48}$$

so that Eq. (47) reduces to

$$\nabla \cdot \mathbf{M}_a = y^2 M_0 \phi'(\phi'' \sin \phi + {\phi'}^2 \cos \phi)$$

$$\times \sin \phi \cos \phi$$
. (49)

We must now digress a moment to recall Thompson's theorem which states that the integral $(8\pi)^{-1} \int \int \mathbf{H}^2 dx \, dy \, dz$ is an upper bound on the stray-field energy even if Eq. (2) is not satisfied, as long as Eq. (3) is satisfied.²⁰ To obtain an upper bound on the correction in energy, we take the correction to \mathbf{H} to have only an x-component, H_x ; this will not mix with the zero-order approximation of Eq. (25) which has only a y-component.

By following this procedure and substituting Eq. (31) into Eq. (49) in the small-angle approximation, one finds for $(8\pi D)^{-1} \int_{-\infty}^{\infty} dx \int_{0}^{D} dy \ H_{x}^{2} dx \ dy$ an upper bound expressible in the form

$$\frac{\pi}{5} \left(\frac{D^2 M_0^2}{\mu} \right) \left(\frac{D^2 K}{\mu} \right) \left(\frac{A}{\mu} \right) (K\mu)^{\frac{1}{2}}$$

$$\times \int_0^{\infty} dV (1 + V^2)^{-3/2}, \qquad V^2 = \mu \phi^2 / A,$$

which is seen to be small compared to Eq. (42), if we note Eq. (43), under usual circumstances, and is seen to vanish with A.

Assumption 3. This assumption is found to be valid as long as b+D is small compared to $(A/K)^{\frac{1}{2}}$ (see, for example, Eq. (31)). However, if only the weaker condition (44) is satisfied, rapid variations near the plane x=0 ensue when $A\to 0$. The consequences are assessed in connection with Assumptions 2, 5, and 6.

Assumption 4. We have no estimate of the error in energy introduced by this assumption. It could be investigated only with a great deal of additional effort because the variation of small corrections to our calculated $\phi(x)$ and $M_{\nu}(x, y)$ gives rise to partial differential equations in two dimensions with variable coefficients.

Assumption 5. A lengthy analysis suggests that the correction to the stray-field energy calculated in the "capacitor" approximation of Section 2 is smaller by a factor on the order $b[(K/A)^{\frac{1}{2}} + (K/\mu)^{\frac{1}{2}}]^{-1}$. Since this conclusion is plausible, the argument will not be reproduced. Also, we may again invoke Thompson's theorem20 to argue that our result constitutes an exact upper bound of the stray-field energy for the given M distribution because H satisfies Eq. (3) and continuity requirements exactly. Thus, since a lower bound on the density $(H^2/8\pi)$ is zero, we know that the discontinuity in $M_{x,x}$ at x = 0 which appears in the limit $A \rightarrow 0$ does not contribute a non-physical infinity to the energy. The only effect of the discontinuity can be to reduce the stray-field energy in a region near x = 0, and it is difficult to see how this region could extend much beyond |x| = b to give a correction greater than $b[(K/A)^{\frac{1}{2}} + (K/\mu)^{\frac{1}{2}}]^{-1}$.

Assumption 6. To test this assumption we calculate the dominant contribution

$$Q = 2\tilde{A}D^{-1} \int_{0}^{\infty} dx \int_{0}^{D} dy M_{y,x}^{2}$$
 (50)

to the energy per unit area mentioned above in the discussion of Assumption 2. Using again Eqs. (48) and (31) in the small ϕ approximation as in discussing Assumption 2, we find that

$$Q = \frac{2KD^2}{3\mu} (K\mu)^{\frac{1}{2}} \int_0^\infty dV (1 + V^2)^{-7/2}, \tag{51}$$

which is a negligible correction to Eq. (42) under condition (44).

Having shown that our series of assumptions is internally consistent under the condition (44), we now consider the conditions on film parameters implied by condition (44). To keep things simple we consider only the case $k_{\perp}=0$.

According to Eqs. (28) and (22), we have the condition $\mu \gg A$ as long as

$$(bD)^{\frac{1}{2}} \gg \lambda \sim 40 \text{ Å(permalloy)}.$$
 (52)

Since condition (52) is satisfied in most permalloy experiments we may use Eq. (43) to reduce condition (44) to

$$M_0(bD/K)^{\frac{1}{2}} \gg b + D.$$
 (53)

This can be re-expressed in the form

$$\frac{K}{M_0^2} \ll \frac{b}{D} \ll \frac{M_0^2}{K} \sim 10^3 \text{(permalloy)}. \tag{54}$$

Thus we see that our approximation from 13, which finally neglects exchange altogether and whose results are represented be Eqs. (40), (42), and (43), is adequate over a broad range of circumstances. The additional details of the present paper are relevant to investigation of the wall-shape in the kernel region and also in situations in which k_{\perp} and/or A/μ are appreciable.

· Comparison with experiment

The shape of a double-film wall in permalloy with an SiO intermediate layer has been measured by Feldtkeller et al.²¹ by means of an electron-microscope technique. In comparing the results with theory, it is convenient to begin by considering the slope of the wall at the center, the reason being that this quantity does not involve the coupling μ . We set $\phi = 0$ in Eq. (31) to find

$$\phi'^2 = K/A \qquad (\phi = 0).$$
 (55)

The experimental slope taken from Abb. 7 of Feldtkeller et al.²¹ appears to be about

$$\phi' = 4.3 \times 10^{-4} \, \text{radian/Å}, \quad (\phi = 0),$$
 (56)

and the anisotropy is reported to be $K = 1.2 \times 10^3$ erg/cc. Substituting these values into Eq. (55) we find that

$$A = 0.65 \times 10^{-6} \text{ erg/cm}.$$
 (57)

This value of exchange is consistent with values of 0.55×10^{-6} and 1.0×10^{-6} erg/cm determined by the resonance method in films of permalloy composition (80 Ni, 20 Fe and 81 Ni, 19 Fe).¹⁹

Using these values of A and K we plot, in Fig. 3, the experimental data of Feldtkeller *et al.* (dashed curves). We see that, just as Feldtkeller *et al.* remarked, the wallshape for a double film has nearly the bulk Bloch form $(\mu/A=0)$, in Fig. 3), and shows experimentally undetectable evidence of distortion by stray fields. For the sake of comparison, an experimental Néel wall shape for a single film of the same thickness is also shown in Fig. 3.

Other experimental values reported by Feldtkeller et al. are D=350 Å, and b=100 to 200 Å. Assuming $M_0=800$ gauss and neglecting k_\perp , we find from Eqs. (28) and (29) that μ/A lies between 12 and 22, depending on the value of b. But we see that the theoretical curve $\mu/A=10$ in Fig. 3 is already somewhat different in the flank region from the experimental curve. However, Dr. Feldtkeller has stated privately that the experimental error is too great to distinguish the case $\mu/A=0$ from $\mu/A=10$. Thus, the experiment is consistent with theory but its accuracy is insufficient to confirm the predicted effect of the coupling.

It may be useful to indicate in the context of these experimental values the potential importance of perpendicular anisotropy. In order to reduce μ to the vicinity of zero, a value in the neighborhood of $k_{\perp} = 10b/D = -3$

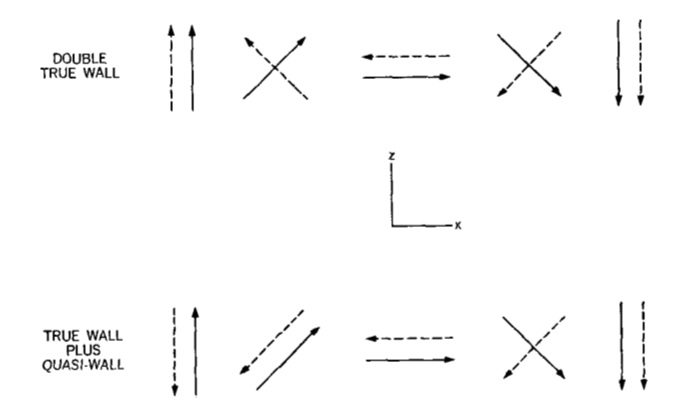


Figure 4 Schematic illustration of distinction between a true wall and a quasi-wall. The solid arrows represent the projection on the film plane of the magnetic configuration in a true wall within one magnetic film. The dashed arrows indicate the configuration, in a second film, for a true wall (above) and a quasi-wall (below).

to -6 would be required. Experiments of Fujiwara *et al.*¹⁸ reveal values of k_{\perp} ranging between 0 and -4 for Ni 80, Fe 20, depending on substrate temperature and pressure in the vacuum chamber during deposition. Since some of these values fall within the required range, we see that perpendicular anisotropy may play a crucial role in determining the wall structure. In fact, if $-k_{\perp}$ is great enough, $\mu + A$ becomes negative and the state of uniform magnetization ($\phi = \pm \pi/2$) is unstable (See Eq. (27)). One expects in this case spatially periodic distributions of magnetization analogous to stripe-domains in single films.¹⁷ This problem, however, is beyond the scope of the present paper.

It appears that further experiments are needed, along with independent determinations of k_{\perp} , to adequately test the theoretical wall shape.

Quasi-walls

Most of Middelhoek's observations^{5,10,14} pertain not to double walls in the strict sense of Fig. 1 but to a configuration consisting of a true wall in one film coupled to a "quasi-wall" in the second film. In the quasi-wall the magnetization rotates from 0 to 90° (or nearly 90°) on one side of the center and then back to 0°, rather than to 180°, on the other side. This distinction is illustrated schematically in Fig. 4. The stability of a quasi-wall opposite a true Néel wall arises from the fact that it closes the pattern of flux coursing through the Néel wall. Under appropriate circumstances, the attendant decrease in magnetostatic energy more than compensates for the anisotropy and exchange in the quasi-wall.

We can argue that in the limit $A/\mu \to 0$ the energy of a double true-wall is equal to that of a true-wall-quasi-wall configuration. To show this, we construct a trial function

for the latter configuration from our solution to the former one by reversing the sense of rotation of \mathbf{M} in one-half of the wall in *one* of the two magnetic films. That is to say, we let

$$\phi \rightarrow -\phi \quad \text{for} \quad \phi > 90^{\circ} \,.$$
 (58)

This is equivalent to replacing $M_z \to -M_z$ for x > 0. This change, one finds, alters *none* of the energy terms. However, the symmetry of Assumption 1 is now broken with respect to exchange considerations because the discontinuity in ϕ' at $\phi = 0$ within the quasi-wall may be smoothed over to reduce $A \int \phi'^2 dx$. But we have assumed already that exchange energy is negligible so this potentiality for energy gain must also be negligible because $A \int \phi'^2 dx$ is positive definite.

With respect to the remaining magnetostatic and anisotropy terms, the transformation (58) presents no new opportunity for reducing the energy since neither of these terms depends on M_z . Since M_x and M_y are independent field variables and M_z is absent altogether, **M** must be in equilibrium again, given the boundary condition $|M_x|$ = M_0 at x = 0. Of course, this condition does not hold within the quasi-wall in an exact description. Nonetheless our limit of $t \gg b + D$ requires $|M_x|$ to be the same in both films in order to optimize flux closure, thereby guaranteeing this condition within both films. Thus our simplified results for the limit $A/\mu \rightarrow 0$, represented by the Eqs. (40) and (42), with μ given by Eq. (28) (and A = 0), apply to a real-wall-quasi-wall configuration under the same conditions of validity described above. Similar ideas form the basis of Middelhoek's discussion of quasi-wall effects in film pairs with unequal as well as equal film thickness.¹⁴

We may add that all of our calculated results (for finite A as well as vanishing A) and preceding considerations hold equally well for a domain wall in a film of thickness D separated by a distance b/2 from an infinitely thick slab composed of material with infinite magnetic susceptibility. This fact is seen by considering the lower surface of the slab to lie on the plane y = D + b/2 in Fig. 1. Our field distribution calculated for $y \le D + b/2$ (as well as the exact distribution) satisfies the required condition that the tangential components of H vanish at the surface of a perfect magnet. All else follows as before.

• Extensions to three or more magnetic films

We can argue that our solution applies to a certain class of wall problems involving three or more magnetic films. Figure 5 shows a multiple-layer structure constructed by piling any number of double films one upon another. This construction produces a structure in which the outermost magnetic films have thickness D and the interior magnetic films have thickness D. All of the non-magnetic layers have the same thickness D. The complex wall consists entirely of true walls, each of which shares its flux

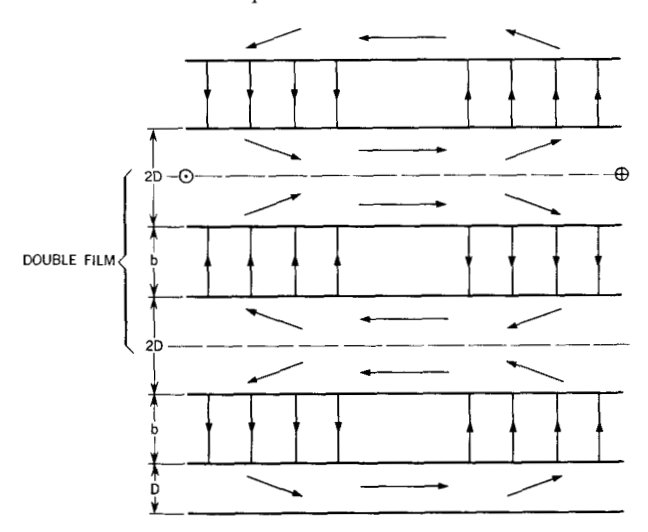
equally with its nearest neighbors. The x and y components of **H** and **M** are indicated schematically in Figure 5.

From symmetry considerations it follows that the quantities $\partial H_x/\partial y$, H_y , $\partial M_x/\partial y$, and M_y must all vanish at the planes indicated by dashed lines in Fig. 5, where one double film touches another. But these conditions are already satisfied within the approximations of our general solution of the double-film problem. It follows that the Eqs. (8), (24), (34) and (37) for energy and wall-shape apply to this problem as well. In fact the results are even more accurate for this multiple-film problem because less external field energy is neglected. The energy given by Ref. 8 for this problem is a factor of the order a/(b+D) greater than ours because the flux is allowed to close only at the edges of the walls rather than throughout their thickness.

A stable wall structure involving quasi-walls may be constructed from the multiple true-wall structure by replacing some of the true walls by quasi-walls. Our double-wall conclusions for the limiting case $A/\mu \to 0$ apply equally well to this case. One can easily convince himself, however, that such a structure cannot be stable if two quasi-walls are adjacent because the energy can be decreased monotonically by a continuous deformation, independent of z, which eliminates them.

We might also say something about the case in which only one of the several magnetic layers has a true domain wall, the others having only the quasi-walls required by flux closure. It is evident that only the nearest-neighbor layers are needed to close the flux. Although the structure

Figure 5 Schematic representation of a wall configuration in a multiple film generated by piling several double films upon each other. Only x and y components of H and M are indicated by the arrows. The sense of M_z depends on whether true walls or quasi-walls are involved.



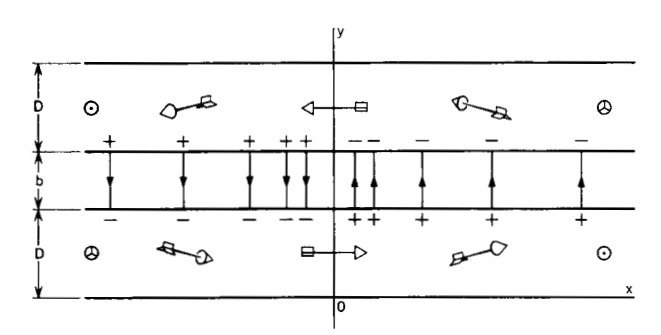


Figure 6 Schematic configuration of a hypothetical double true-wall of a second kind, as distinguished from the first kind shown in Fig. 1.

is now not given correctly by our general theory, the limit $A/\mu \to 0$ $k_\perp \to 0$ is still applicable.

• Exchange-like coupling

Experiments of Bruyère et al.²² have disclosed that a double magnetic film utilizing a very thin metallic non-magnetic intermediate layer shows evidence of an exchange-like interaction between the two magnetic films. Within the limits of our approximations, $|M_y| \ll M_0$ and $\phi = \phi(x)$, the additional energy \mathcal{L}_{ϵ} may be written in the form

$$\mathcal{L}_{\epsilon} = -C \cos \left(\phi_1 - \phi_2 \right), \tag{59}$$

where $\phi_1 \equiv \phi$ is the orientation of **M** in film 1 and ϕ_2 is the orientation of **M** in film 2. We make no assumption about how the coefficient C depends on film thicknesses or other parameters. However, we note in passing that the experimental values of C are positive ("ferromagnetic" coupling).

In the case of the true-wall structure of Fig. 1 with domains in both films similarly magnetized, we have the condition

$$\phi_1 + \phi_2 + \pi = 0, \tag{60}$$

and Eq. (59) becomes

$$\mathcal{L}_{e} = C \cos 2\phi = -C + 2CM_{x}^{2}/M_{0}^{2}. \tag{61}$$

When this term is included in Eq. (1), we see that nothing is changed in the theory except that K is replaced by K + 2C. (Feldtkeller drew the same conclusion with respect to his theory⁷).

We can also hypothesize the true-wall structure of a second kind, one represented by Fig. 6. Its existence has not, to the author's knowledge, been positively established by experiment. Here we have

$$\phi_2 = \phi_1 + \pi, \tag{62}$$

and therefore

$$\mathcal{L}_{\epsilon} = C, \tag{63}$$

and the wall structure is not changed. However, if C > 0, then the energy is at most a relative minimum because the operation $\phi_2 \to -\phi_2$ will decrease the domain energy density by an amount 2C.

Finally, a real-wall-quasi-wall structure cannot find an equilibrium in the presence of exchange coupling since it gains an energy of 2C per unit volume of magnetic material swept out if the wall is displaced.

Acknowledgments

The author is indebted to S. Middelhoek for many stimulating and informative discussions, and to F. Friedlaender, E. Kneller, A. Aharoni, and E. Feldtkeller for helpful comments during the course of this work.

References

- W. Ruske, Monatsber. d. Deutsch. Ak. d. Wiss. (Berlin) 2, 161 (1960).
- 2. H. Clow, Nature 194, 1035 (1962).
- I. B. Puchalska and R. J. Spain, Compt. Rend. 254, 2937 (1962).
- H. W. Fuller and D. J. Sullivan, J. Appl. Phys. 33, 1063 (1962);
 H. W. Fuller and L. R. Lakin, J. Appl. Phys. 34, 1069 (1963).
- 5. S. Middelhoek, Z. Angew. Phys. 18, 524 (1965).
- J. C. Slonczewski and S. Middelhoek, Appl. Phys. Lett. 6, 139 (1965).
- 7. E. Feldtkeller, Z. Angew. Phys. 18, 532 (1965).
- F. J. Friedlaender, E. Kneller, and L. F. Silva, *Intermag.* (1965); L. F. Silva, thesis, Purdue University, 1965;
 F. J. Friedlaender and L. F. Silva, to be published.
- F. J. Friedlaender and L. F. Silva, J. Appl. Phys. 36, 946 (1965).
- 10. S. Middelhoek, Appl. Phys. Letters 5, 70 (1964).
- 11. S. Middelhoek, IBM Journal 9, 147 (1965).
- C. E. Patton and F. B. Humphrey, J. Appl. Phys. 37, 1270 (1966).
- 13. J. C. Slonczewski, J. Appl. Phys. 37, 1268 (1966).
- 14. S. Middelhoek, J. Appl. Phys. 37, 1276 (1966).
- 15. E. Feldtkeller, Göttinger Akademie der Wissenschaften.
- W. F. Brown, Jr., Micromagnetics, John Wiley and Sons, New York, 1963.
- R. J. Spain, Appl. Phys. Letters 3, 208 (1963).
 N. Saito,
 H. Fujiwara, and Y. Sugita, J. Phys. Soc. Japan 19, 421 (1964);
 19, 1116 (1964); Appl. Phys. Letters 4, 160 (1964).
- S. Fujiwara, T. Koikeda, and S. Chikazumi, J. Phys. Soc. Japan 20, 878 (1964); T. Koikeda and S. Chikazumi, J. Phys. Soc. Japan 21, 399 (1966).
- See, for example, M. Prutton, Thin Ferromagnetic Films, Butterworth, 1964.
- See, for example, W. F. Brown, Jr., J. Phys. Soc. Japan 17, 540 (1962).
- E. Feldtkeller, E. Fuchs, and W. Liesk, Z. Angew. Phys. 18, 370 (1965).
- J. C. Bruyère, O. Massenet, R. Montmory and L. Néel, C. R. Acad. Sci. (Paris) 258, 841 and 1423 (1964); Intermag. (1964) Proceedings 16-1.